Highly tunable large-core single-mode liquid-crystal photonic bandgap fiber

Thomas Tanggaard Alkeskjold, Jesper Lægsgaard, Anders Bjarklev, David Sparre Hermann, Jes Broeng, Jun Li, Sebastian Gauza, and Shin-Tson Wu

We demonstrate a highly tunable photonic bandgap fiber, which has a large-core diameter of 25 μm and an effective mode area of 440 μm^2. The tunability is achieved by infiltrating the air holes of a photonic crystal fiber with an optimized liquid-crystal mixture having a large temperature gradient of the refractive indices at room temperature. A bandgap tuning sensitivity of 27 nm/°C is achieved at room temperature. The insertion loss is estimated to be less than 0.5 dB and caused mainly by coupling loss between the index-guided mode and the bandgap-guided mode. © 2006 Optical Society of America

OCIS codes: 230.3990, 060.2310.

1. Introduction

Photonic crystal fibers (PCFs), also known as microstructured optical fibers, have an arrangement of micrometer-sized air holes running down the length of the fiber. The microstructure allows realization of so-called index-guiding PCFs, which guide light in a high-index core by using a principle similar to total internal reflection, and bandgap-guiding PCFs, which can guide light in a low-index core by coherent reflection from a surrounding periodic microstructure. The latter type guides light within certain spectral bands formed by the periodic microstructure, which surrounds a low-index core. Further, the presence of air holes in PCFs has also given the possibility of infusing liquids into the fiber and this has opened up the possibility of creating tunable fibers and tunable fiber-based devices for tuning, trimming, scrambling, and controlling, for example, dispersion, polarization, and attenuation by using both index-guiding[1–3] and bandgap-guiding fibers.[4–8] It has previously been demonstrated that an initial index-guiding PCF can be converted to a highly tunable bandgap-guiding-type PCF by infiltrating the air holes with suitable liquid crystals (LCs), which allow for thermal[5], electrical,[6,8] and all-optical tuning.[7] The spectral properties of these types of fiber can be described by using an antiresonant model, which predicts the spectral stopbands to be positioned at wavelengths corresponding to modal cutoff wavelengths of a single liquid-filled air hole,[9,10] which make up a traditionally index-guiding waveguide. The spectral properties of LC PCFs can be thermally tuned by using LCs having nematic, smectic A, and cholesteric mesophases, which yield different functionalities such as threshold switching and tunable spectral filtering[5]. In the latter case, thermally shifting the bandgaps can, for example, be achieved by utilizing the temperature dependence of the ordinary refractive index, dn_0/dT, of nematic LCs by resistive or optical pump-induced heating.[7] In this case it is desirable to have a high tuning sensitivity at approximately room temperature in order to decrease the power consumption and ease handling and packaging. To achieve a large dn_0/dT at room temperature, a high birefringence and low clearing temperature are crucial LC parameters. These two requirements are often conflicting, but such a LC was recently demonstrated.[11] Furthermore, for applications involving, for example, dispersion trimming of short laser pulses with high peak power, it is desirable to use single-mode PCFs having a very large mode area in order to have a low fraction of the field propagating in the LC. Here we present a tunable large-core single-

T. T. Alkeskjold (ttl@com.dtu.dk), J. Lægsgaard, and A. Bjarklev are with the Department of Communications, Optics, and Materials, Technical University of Denmark, DK-2800 Lyngby, Denmark. D. S. Hermann is with the Department of Microtechnology and Nanoscience MC2, the Photonics Laboratory, Chalmers University of Technology, 41296 Gothenburg, Sweden. J. Broeng is with Crystal Fibre A/S, Blokken 84, DK-3460 Birkerød, Denmark. J. Li, S. Gauza, and S.-T. Wu are with the College of Optics and Photonics [CREOL and Florida Photonics Center of Excellence (FPCE)], University of Central Florida, Orlando, Florida 32816.

Received 13 June 2005; revised 28 September 2005; accepted 10 October 2005.

0003-6935/06/102261-04$15.00/0

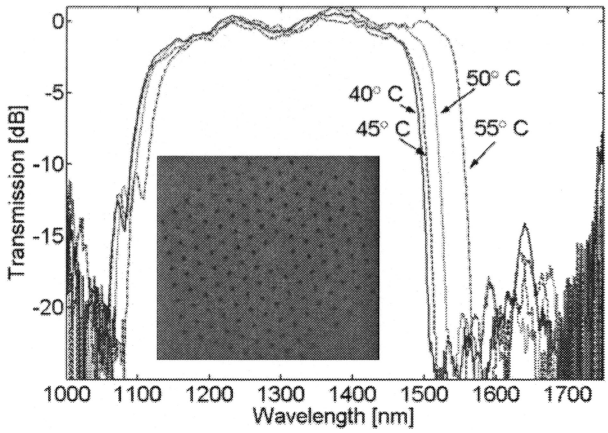

Fig. 1. Transmission spectrum for the three-rod core PCF, where the air holes have been filled for 10 mm of the length with the nematic LC E7 (Merck, Darmstadt, Germany). Inset, optical micrograph of the PCF end facet. Hole diameter and interhole distance is 2.9 and 11.2 μm, respectively.

mode photonic bandgap fiber, which has a core diameter of 25 μm, an effective mode area of 440 μm^2, and a high tuning sensitivity around room temperature. This is achieved by using a specially synthesized nematic LC (Ref. 11) and a three-rod core PCF.[12]

2. Device Characterization

In this experiment we used 2 m of a so-called LMA25 PCF, where the core is surrounded by six rings of air holes arranged in a triangular lattice (Fig. 1, inset). The hole diameter (d), interhole distance (Λ), core size, and outer diameter were 2.9, 11.2, 25, and 470 μm, respectively. The large mode area is obtained by using a three-rod core design.[12] The endlessly single-mode property for index guiding is retained by scaling the relative hole diameter to $d/\Lambda = 0.26$, which is slightly larger than the theoretical limit of 0.25. High leakage and bend loss were observed for $\lambda < 1$ μm due to the relatively small air holes.

A. Low-Gradient Tuning

First, to compare the device with a device based on an existing commercial LC, the air holes were filled with the commercially available nematic LC E7 (Merck, Darmstadt, Germany) for 10 mm of the length using capillary forces. The LC was heated to an isotropic phase and cooled down again slowly to achieve a homogeneous alignment. Polarized microscopy observations on a single silica capillary tube, with an inner diameter of 6 μm, indicated that the LC was planar aligned, i.e., with the LC director aligned along the fiber axis, and therefore with the ordinary index (n_0) predominantly determining the spectral features of the fiber.[6,7]

Figure 1 shows the transmission spectrum at temperatures between $T = 40$ °C and 55 °C in steps of 5 °C. The transmission spectrum was obtained by butt coupling an endlessly single-mode PCF with a 10 μm core diameter to both ends of the LMA25. White light from a halogen–tungsten white light source was coupled into one end and the transmission spectrum was recorded by an optical spectrum analyzer (ANDO AQ6317B) and normalized to the spectrum of an unfilled fiber. The LCPCF was placed in an aluminum block, which was mounted on a Linkam hot stage (MC60 + TH60). The bandgap centered at approximately $\lambda = 1300$ nm has a bandwidth of 345−410 nm, which depends on temperature. As the temperature is increased, the center wavelength of the bandgap shifts toward a longer wavelength due to a positive dn_0/dT, which increases as the clearing temperature of E7 is approached ($T_c = 58$ °C). At the same time, the bandwidth of the bandgap increases, which implies that the shorter and longer bandgap edge experience a different shift, i.e., the long-wavelength edge experiences a larger shift than the short-wavelength edge. The difference in tuning sensitivity between the short- and the long-wavelength bandgap edge can be attributed two mechanisms. First and overall an increase of the refractive index will cause both of the bandgap edges to shift toward longer wavelengths with an equal relative shift, thereby implying a longer absolute shift of the long-wavelength bandgap edge compared to the short-wavelength edge. Second, with increasing temperature the LC will exhibit a reduction of anisotropy, which will cause the bandgap edges to shift differently depending on the transversal and longitudinal distribution of the electric field of the cladding modes, which define the bandgap edges, and thereby exhibit different sensitivity to the LC anisotropy. The tuning sensitivity at 52.5 °C was measured at the long-wavelength edge of the bandgap to be 7 nm/°C or 0.46% per °C when normalized to the center wavelength at the bandgap edge.

The small transmission peak at 1650 nm is a direct feature of the LC anisotropy, which causes a splitting in the effective index of the TE_{01} and the TM_{01} cladding states supported by a LC infiltrated microchannel. The splitting is observed since the electric field of the TE_{01} is solely in the transversal direction, while the TM_{01} has a part of the electric field in the longitudinal direction. The TM_{01} mode therefore experiences the extraordinary index of the LC and a gap in the effective index is formed between the bands derived from the TE_{01} and TM_{01} cladding states. Simulations using the refractive indices of E7 presented in a previous publication[7] confirmed the presence of a guided mode in this bandgap. The simulations were performed by solving the wave equation using a home-developed plane-wave tool, expanding the vectorial magnetic field of the eigenmodes in plane waves, and by using a tensorial dielectric function as described by Meade *et al.*[13,14] and Johnson and Joannopoulos.[15] A supercell consisting of 8×8 elementary cells of the periodic cladding structure is used. Supercell convergence was enhanced by use of a coupling-reducing k point.[16]

The insertion loss of the LC device was difficult to establish exactly due to Fabry–Pérot effects between the two end facets forming the butt coupling, which causes ripples in the transmission spectrum. We es-

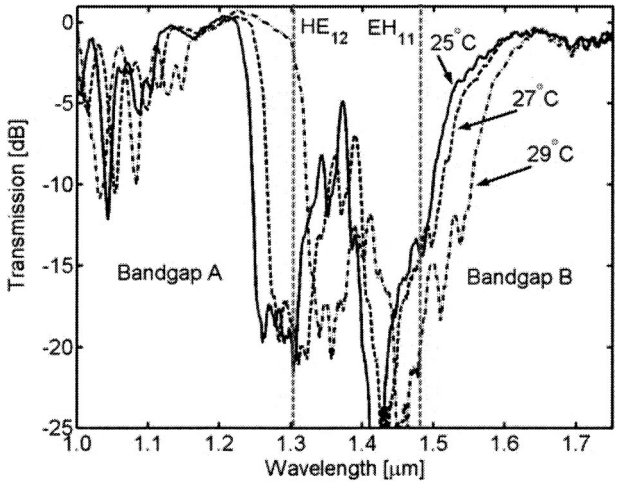

Fig. 2. Temperature-dependent transmission spectra for the three-rod core PCF, where the air holes have been filled for 10 mm of the length with UCF-1.

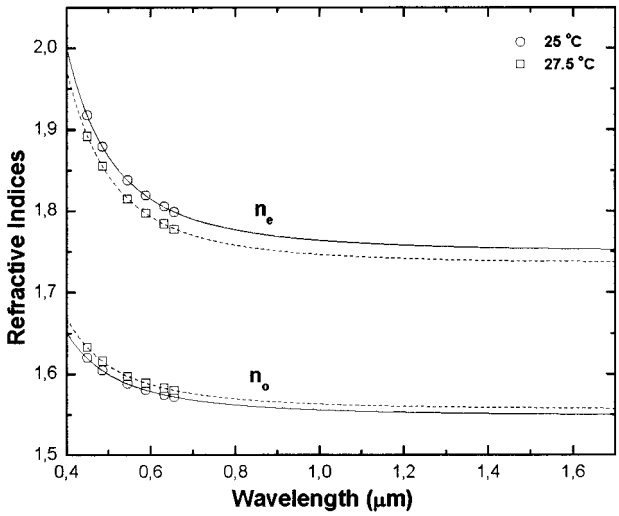

Fig. 3. Wavelength- and temperature-dependent refractive indices n_e and n_o of UCF-1 at $T = 25$ °C and 27.5 °C. Circles and rectangles are measured refractive indices at $\lambda = 450$, 486, 546, 589, 633, and 656 nm and at $T = 25$ °C and 27.5 °C, respectively. Solid and dashed curves are fitting curves to the extended Cauchy equation. The fitting curves are extrapolated to the infrared region based on the experimental data measured in the visible spectral region.

timate the loss to be less than 0.5 dB near the center of the bandgap.

B. High-Gradient Tuning

The tuning sensitivity at room temperature can be increased by using an optimized LC mixture, which has high dn_0/dT at room temperature. Therefore another LCPCF sample was prepared by using the same approach as with E7 but with the nematic LC mixture UCF-1.[11] Polarized microscopy observations on a single capillary tube with UCF-1 also indicated a planar alignment of the LC director. Figure 2 shows the transmission spectrum for the filled PCF. The spectrum shows high transmission in two bandgaps: bandgap A centered at approximately 1150 nm and bandgap B centered at approximately 1700 nm. In between these two bandgaps, a weaker transmission peak appears. This feature is also a direct consequence of the LC anisotropy, which causes a splitting of the EH_{11} mode of an LC-infiltrated microchannel from the HE_{12} and HE_{31} modes,[17] so that a narrow bandgap opens up between the cladding states derived from these modes. Simulations confirmed this and the modal cutoff wavelengths of the EH_{11} and HE_{12} modes, which represent the stopbands in the antiresonant model, are also plotted for $T = 25$ °C in Fig. 2. As observed from Fig. 2, the width and transmission of the bandgap is reduced as the temperature of UCF-1 is increased, which is due to a decreasing anisotropy as the temperature approaches the clearing temperature of UCF-1 ($T_c = 29.7$ °C), whereby the splitting of the EH_{11}, HE_{12}, and HE_{31} cladding modes is diminished. The refractive indices of UCF-1 are shown in Fig. 3 and were measured using a "multiwavelength Abbe refractometer," Atago DR-M4, and fitted using the extended Cauchy equations.[18] Figure 4 shows a comparison between the measured normalized transmission spectrum of bandgap B and the simulation of two times the coupling loss between the index-guided mode (unfilled PCF) and the bandgap-guided mode (LC filled PCF) evaluated by using overlap integrals and the refractive indices of UCF-1 shown in Fig. 3. The insets show simulated mode fields of the index-guided mode in an unfilled PCF (TIR mode), and a PBG guided mode at the center and at the short-wavelength edge of the bandgap. The mode profiles have been normalized to equal intensity and to exhibit the same contour levels. The simulated coupling loss agrees well with the shape of the PBG spectrum, and it is therefore concluded that coupling loss (<0.5 dB) is the dominant loss mechanism, as was also found by Steinvurzel *et al.*[19] The deviation at $\lambda > 1.65$ μm is caused by temporal intensity fluctuations of the halogen–tungsten white light

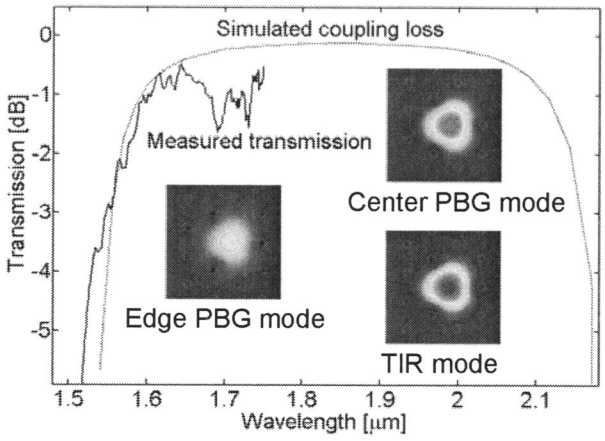

Fig. 4. Transmission spectrum of the UCF-1 filled PCF (solid curve) and simulated coupling loss (dotted curve) from the index-guiding to the bandgap-guiding part of the PCF. Insets show an index-guided mode and PBG guided modes at the bandgap center and edge. The mode profiles have been normalized to equal intensity and to exhibit the same contour levels.

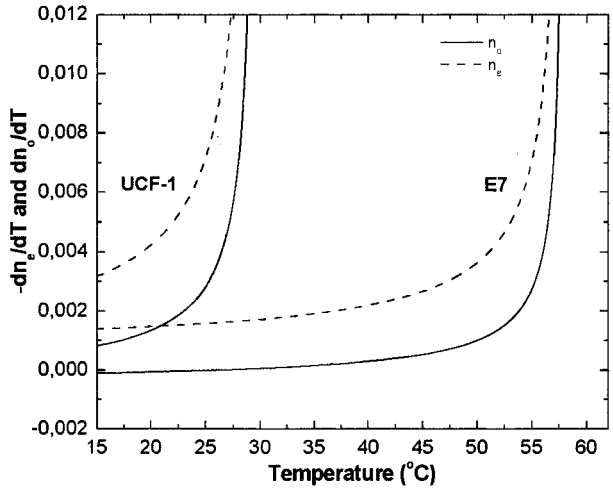

Fig. 5. dn_o/dT and $-dn_e/dT$ for E7 and UCF-1 calculated at λ = 589 nm.

source. In the center of bandgap B, simulation showed that only 0.4%–0.5% of the field energy was propagating in the LC, while simulation on a LC infiltrated single-rod core PCF with d = 3 μm and Λ = 7 μm (Ref. 7) indicated that approximately 4%–5% of the field was propagating in the LC. This indicates that the interaction of field and LC can be reduced by 1 order of magnitude by using a three-rod core design and reducing the relative hole size, while retaining high spectral tuning sensitivity. The spectral tuning sensitivity of the UCF-1 infiltrated PCF at 28 °C was measured at the long-wavelength edge of bandgap A to be 27 nm/°C or 2.1% when normalized. The tuning sensitivity at room temperature when using UCF-1 is therefore approximately 4.6 times higher than when using E7 above 50 °C which is directly related to a higher temperature gradient of UCF-1 at room temperature compared to E7 as shown in Fig. 5. The temperature gradient at λ = 589 nm was calculated by using a four-parameter model[20] for describing the temperature effect on the LC refractive indices. The four parameters were gained by fitting the temperature-dependent LC refractive indices measured at temperatures from 15 to 55 °C at 5 °C intervals and at λ = 589 nm.

3. Conclusion

A highly tunable single-mode photonic bandgap fiber device has been demonstrated, which utilizes a three-rod core PCF and a specially synthesized LC in order to obtain a large mode area and high tuning sensitivity. The guided mode has an effective area of 440 μm^2 with a device insertion loss of less than 0.5 dB. The loss is mainly attributed to coupling losses between the index-guided section and the bandgap-guided section. The thermal tuning sensitivity of the spectral position of the bandgap was measured to 27 nm/°C, which is 4.6 times higher than with commercially available LC E7, and is achieved at room temperature.

References

1. B. J. Eggleton, C. Kerbage, P. S. Westbrook, R. Windeler, and A. Hale, "Microstructured optical fiber devices," Opt. Express **9,** 698–713 (2001).
2. C. Kerbage, R. S. Windeler, B. J. Eggleton, P. Mach, M. Dolinski, and J. A. Rogers, "Tunable devices based on dynamic positioning of micro-fluids in micro-structured optical fiber," Opt. Commun. **204,** 179–184 (2002).
3. F. Du, Y. Q. Lu, and S. T. Wu, "Electrically tunable liquid-crystal photonic crystal fiber," Appl. Phys. Lett. **85,** 2181–2183 (2004).
4. R. T. Bise, R. S. Windeler, K. S. Kranz, C. Kerbage, B. J. Eggleton, and D. J. Trevor, "Tunable photonic band gap fiber," in *Optical Fiber Communication Conference Technical Digest,* Vol. 70 of OSA Trends in Optics and Photonics (Optical Society of America, Washington, D.C., 2002), pp. 466–468.
5. T. T. Larsen, A. Bjarklev, D. S. Hermann, and J. Broeng, "Optical devices based on liquid crystal photonic bandgap fibres," Opt. Express **11,** 2589–2596 (2003).
6. M. W. Haakestad, T. T. Alkeskjold, M. D. Nielsen, L. Scolari, J. Riishede, H. E. Engan, and A. Bjarklev, "Electrically tunable photonic bandgap guidance in a liquid crystal filled photonic crystal fiber", IEEE Photon. Technol. Lett. **17,** 819–821 (2005).
7. T. T. Alkeskjold, J. Laegsgaard, D. S. Hermann, A. Anawati, J. Broeng, J. Li, S. T. Wu, and A. Bjarklev," All-optical modulation in dye-doped nematic liquid crystal photonic bandgap fibers," Opt. Express **12,** 5857–5871 (2004).
8. L. Scolari, T. T. Alkeskjold, J. Riishede, A. Bjarklev, D. S. Hermann, A. Anawati, M. D. Nielsen, and P. Bassi, "Continuously tunable devices based on electrical control of dual-frequency liquid crystal filled photonic bandgap fibers," Opt. Express **13,** 7483–7496 (2005).
9. N. M. Litchinitser, S. C. Dunn, P. E. Steinvurzel, B. J. Eggleton, T. P. White, R. C. McPhedran, and C. M. de Sterke, "Application of an ARROW model for designing tunable photonic devices," Opt. Express **12,** 1540–1550 (2004).
10. J. Laegsgaard, "Gap formation and guided modes in photonic bandgap fibres with high-index rods," J. Opt. A Pure Appl. Opt. **6,** 798–804 (2004).
11. J. Li, S. Gauza, and S. Wu, "High temperature-gradient refractive index liquid crystals," Opt. Express **12,** 2002–2010 (2004).
12. N. A. Mortensen, M. D. Nielsen, J. R. Folkenberg, A. Petersson, and H. R. Simonsen, "Improved large-mode-area endlessly single-mode photonic crystal fibers," Opt. Lett. **28,** 393–395 (2003).
13. R. D. Meade, A. M. Rappe, K. D. Brommer, J. D. Joannopoulos, and O. L. Alerhand, "Accurate theoretical analysis of photonic band-gap materials," Phys. Rev. B **48,** 8434–8437 (1993).
14. R. D. Meade, A. M. Rappe, K. D. Brommer, J. D. Joannopoulos, and O. L. Alerhand, "Erratum: Accurate theoretical analysis of photonic band-gap materials," Phys. Rev. B **55,** 15942 (1997).
15. S. G. Johnson and J. D. Joannopoulos, "Block-iterative frequency-domain methods for Maxwell's equations in a plane-wave basis," Opti. Express **8,** 173–190 (2001).
16. M. Albertsen, J. Lægsgaard, S. E. B. Libori, K. Hougaard, J. Riishede, and A. Bjarklev, "Coupling reducing k-points for photonic crystal fiber calculations," Photonics Nanostruct. **1,** 43–54 (2003).
17. J. D. Dai and C. K. Jen, "Analysis of cladded uniaxial single-crystal fibers," J. Opt. Soc. Am. A **8,** 2021–2025 (1991).
18. J. Li and S. T. Wu, "Extended Cauchy equations for the refractive indices of liquid crystals," J. Appl. Phys. **95,** 896–901 (2004).
19. P. Steinvurzel, B. T. Kuhlmey, T. P. White, M. J. Steel, C. M. de Sterke, and B. J. Eggleton," Long wavelength anti-resonant guidance in high index inclusion microstructured fibers," Opt. Express **12,** 5424–5434 (2004).
20. J. Li, S. Gauza, and S. T. Wu, "Temperature effect on liquid crystal refractive indices," J. Appl. Phys. **96,** 19–24 (2004).